The Participatory Universe A Conceptual Framework for Reality as an Observer-Dependent, Sampled Manifestation of Underlying Potential Final

Analytical Formalization and Empirical Validation Proposals

(Version M.A11 - Refined Phase 1 Execution Plan)

May 8, 2025

Abstract

This document details the "Participatory Universe" framework, where finite, quantum reality ($\mathbb{R}_{\mathcal{O}}$) emerges for observers ($\mathcal{O}$) via $f_{s,\mathcal{O}}$-limited sampling of an underlying, unmanifested potential ($\mathbb{X}_{potential}$). Aliasing, a process analogous to the stroboscopic "wagon wheel" effect, via $\text{Map}_{\text{Alias}}$ is hypothesized to generate quantum phenomena and an observer-specific Planck's constant $h_{\mathcal{O}} \propto 1/f_{s,\mathcal{O}}$, potentially resolving classical divergences. This version incorporates a significantly refined and detailed execution plan for Phase 1 of the Research Roadmap (Section 2), focusing on immediate verification of mathematical derivations and development of numerical toy models. It integrates specific analytical derivations and proposals (provided by the user) addressing previous challenges regarding $\mathbb{X}_{potential}$ consistency, the nature and origin of $f_{s,\mathcal{O}}$ and the universal constant κ, measurement dynamics, the Born rule, and inter-observer consistency (Section 9). It also includes enhanced experimental designs for empirical validation via cosmology, quantum optics, and gravity tests (Section 10). While significantly advancing the framework's rigor, verification of its mathematical underpinnings and execution of proposed experiments remain crucial future work requiring expert collaboration. This serves as a comprehensive research proposal [1, 2].

Contents

Preamble: The Co-Creation of Reality

This work explores a paradigm where the experienced universe emerges through co-creation: interactions between an unmanifested Potential ($\mathbb{X}_{potential}$) and Observers ($\mathcal{O}$) characterized by intrinsic sampling rates ($f_{s,\mathcal{O}}$). Much like the familiar 'wagon wheel' effect where a camera's finite sampling rate can create illusory motion from rapid, periodic input, this framework posits that reality and its laws, including Quantum Mechanics (QM), are emergent properties shaped by these fundamental informational limits. This document outlines the framework, presents refined analytical formalizations and derivations (Section 9), details enhanced empirical validation strategies (Section 10), and provides a research roadmap (Section 2) with a detailed action plan for its initial phase.

1 Introduction: The Limits of Current Paradigms and the Need for a New Foundation

Modern physics, encompassing Quantum Mechanics (QM) and General Relativity (GR), faces profound challenges of incompleteness, exemplified by the quantum gravity puzzle, the measurement problem, and the axiomatic nature of fundamental constants like Planck's constant h. Classical physics failures, such as the ultraviolet catastrophe, historically motivated paradigm shifts towards frameworks incorporating inherent resolution limits.

This framework proposes that Reality ($\mathbb{R}_{\mathcal{O}}$) for an Observer ($\mathcal{O}$) is an $f_{s,\mathcal{O}}$-limited, sampled manifestation of an underlying potential $\mathbb{X}_{potential}$. Aliasing via $\text{Map}_{\text{Alias}}$ of details beyond the $f_{s,\mathcal{O}}/2$ Nyquist threshold – a principle familiar from the stroboscopic 'wagon wheel' effect where a camera's finite frame rate can create illusory motion from rapid, periodic input – is hypothesized as the origin of:

- Quantum phenomena (formalized in Sec. 9.2).
- An observer's effective Planck's constant $h_{\mathcal{O}} \propto 1/f_{s,\mathcal{O}}$ (formalized in Sec. 9.3).
- The resolution of classical divergences by providing a natural UV cutoff (Sec. 4.3).

This document details the proposed mathematical structures (Sec. 9) and empirical tests (Sec. 10) aimed at substantiating these claims, acknowledging the significant theoretical and experimental work still required.

2 Roadmap for Advancing the Framework

This roadmap outlines a phased research program, referencing the detailed formalizations (Sec. 9) and validation strategies (Sec. 10). The immediate focus is on Phase 1, detailed below, which aims to establish the mathematical soundness and foundational plausibility of the core mechanisms.

Phase 1: Verification of Formalism and Toy Models (Year 1, Months 1-9 approx.)

- **Overall Goal:** Confirm mathematical consistency of core derivations and demonstrate the emergence of quantum-like phenomena via aliasing in simplified numerical models. This phase addresses the critical challenge of mathematical rigor and builds foundational confidence in the framework.
- **General Approach:** Employ analytical methods (using symbolic math software like Python's SymPy or Mathematica) and numerical simulations (using Python with NumPy, SciPy, Matplotlib). All code, derivations, and results will be documented in Jupyter Notebooks and summarized in technical reports, shared via a public GitHub repository to invite community scrutiny and collaboration.
- **Timeline:** Approximately 6-9 months for initial focused effort by a small team or individual.
- **Key Sub-Phases (Detailed Below):**
  - Phase 1.1: Detailed Verification of Core Mathematical Derivations (Sec. 2.0.1)
  - Phase 1.2: Development and Analysis of Numerical Toy Models (Sec. 2.0.2)
- **Overall Milestone for Phase 1:** Technical report and preprint summarizing verification results and toy model simulations, including any identified inconsistencies or required modifications to the formalism, by Q4 Y1 (e.g., Q4 2025 / Q1 2026).

Phase 2: Refining $f_{s,\mathcal{O}}$ Model and κ Estimation (Year 1-2)

- **Action:** Rigorously develop and test scaling relations for $f_{s,\mathcal{O}}$ (Sec. 9.3, Derivation 9.3), exploring its physical basis (Sec. 4.2). Resolve origin/value of κ (Proposal 9.3) ensuring consistency with $h_{\text{shared}} \approx \hbar$ via convergence mechanism (Sec. 9.6). This includes theoretical work on clarifying the observer concept (Sec. **??**).
- **Goal:** Establish predictive model for $f_{s,\mathcal{O}}$; constrain/derive κ. (Milestone: Consistent model for f_s scaling and κ proposed, white paper on observer definition by Q2 Y2).

Phase 3: Extending Derivations (Year 2-3)

- **Action:** Derive Schrödinger/Dirac dynamics from first principles (Sec. 9.7). Rigorously prove Born rule derivation validity (Derivation 9.4) or develop alternatives. Develop operator algebra. Model $\text{Interact}_{\text{Resolve}}$ dynamics including decoherence (Proposal 9.6, Derivation **??**).
- **Goal:** Demonstrate further QM formalism emergence. (Milestone: Derivation of effective Hamiltonian in toy model by Q4 Y2).

Phase 4: Inter-Observer Consistency Refinement (Year 2-3)

- **Action:** Refine network convergence model (Derivation 9.5) with realistic interactions (W_{ij}). Validate mechanism justifying $\bar{f}_s \approx \kappa/\hbar$ (Proposal 9.7). Analyze stability.
- **Goal:** Provide compelling explanation for universality of $\hbar$. (Milestone: Stability analysis completed by Q3 Y3).

Phase 5: Executing Empirical Tests (Year 3-5)

- **Action (Cosmology):** Perform detailed CMB likelihood analysis vs. derived $C_\ell(n)$ (Experiment 10.1). (Milestone: First CMB constraints on n by Q4 Y3).
- **Action (Lab-scale):** Pursue funding/collaboration for refined quantum optics and gravity tests (Experiments 10.2, 10.3, 10.4), building on preparatory simulations (Sec. **??**). Execute initial experiments. (Milestone: Experimental proposal submitted by Q2 Y4).
- **Action (DM/DE):** Develop specific predictions from sampling effects (Experiment 10.5, Derivation 10.1) and test against data.

2.0.1 Phase 1.1: Detailed Verification of Core Mathematical Derivations (Months 1-4)

Objective: To rigorously test the consistency and robustness of key mathematical derivations presented in Section 9, ensuring a sound mathematical foundation. This addresses the critical challenge of mathematical rigor. **Tools**: Python's SymPy or Mathematica for analytical derivations; Python's NumPy, SciPy for numerical checks; Jupyter Notebooks for interactive exploration; LaTeX for technical reports; GitHub for version control. **Deliverable**: Technical report summarizing verification results, including inconsistencies or required modifications, with code shared on GitHub.

1.1.1: Derivation 9.1 (Measure Consistency for $\mathbb{X}_{potential}$) Verification

- **Context:** The framework posits a Gaussian measure μ on $H^s(\mathbb{R}^m)$ with covariance C (Fourier symbol $|A(\vec{k})|^2 \propto |\vec{k}|^{-\alpha}$). Well-definedness requires C to be trace-class ($\alpha > m$) and the Sobolev norm to be integrable ($\alpha > m + 2s$).

- **Action:**
  - Analytically compute $\int |\vec{k}|^{-\alpha} d^m \vec{k}$ for $m = 1, 2, 3$ using polar coordinates to confirm $\alpha > m$.
  - Analytically verify $\int (1 + |\vec{k}|^2)^s |\vec{k}|^{-\alpha} d^m \vec{k} < \infty$ for $\alpha > m + 2s$, considering typical s values (e.g., $s = 1, 2$).
  - Numerically cross-check analytical integrals using 'scipy.integrate.quad' for edge cases (e.g., $\alpha \approx m$). (See repository for code, e.g., 'trace$_c lass_c heck.py$').$Testalternatives$ (e.g., exponential decay $e^{-\beta|\vec{k}|}$, Gaussian decay $e^{-\beta|\vec{k}|^2}$) by recalculating convergence conditions. Specify β for comparability (e.g., matching variance).

–

Justify the choice of singularity handling at $k = 0$ (e.g., cutoff ϵ, physical regulators) and quantify sensitivity.

Ensure the choice of Sobolev regularity s is physically motivated.

Document whether alternative spectra preserve key framework predictions (e.g., aliasing behavior).

1.1.2: Derivation 9.2 (Hilbert Space and Interference) Verification

- **Context:** The aliasing map $\text{Map}_{\text{Alias}}$ with a sharp band-pass kernel K is claimed to map $\Phi \in H^s(\mathbb{R}^m)$ to $\psi_{\mathcal{O}} \in \mathcal{H}_{\mathcal{O}} \cong L^2(\mathbb{R}^3)$ and produce interference $\Delta x \propto 1/f_{s,\mathcal{O}}$.
- **Action:**
  - Verify Hilbert space properties (linearity, L^2 integrability via Paley-Wiener, completeness as a closed subspace of L^2).
  - Analytically calculate the 1D interference pattern for $\Phi(z)$ modeled as two narrow Gaussians. Specify a model for $\vec{z}_{proj}$ (e.g., identity for $m = 3$) and test its impact.
  - Numerically compute $\psi_{\mathcal{O}}$ for a simple Φ and verify interference, estimating fringe spacing. (See repository for code, e.g., 'interference$_s im.py$').$Testsensitivitytokernelch$ $passkernelwithaGaussianwindowedkernel : K_G(\vec{k}) \propto e^{-|\vec{k}|^2/(f_{s,\mathcal{O}}/2)^2}$.
  - Verify the uncertainty principle derivation.

Clarify how $\vec{z}_{proj}$ assumptions affect interference.

Assess effects of different kernels on fringe sharpness and aliasing artifacts.

Ensure numerical stability in kernel computations (e.g., near $x = z$).

1.1.3: Derivation 9.4 (Born Rule Uniformity) Verification

- **Context:** The Born rule $P_i \propto |c_i|^2$ is claimed if aliased power $\mu_i = \sum_n |A(\vec{k}_i + nf_{s,\mathcal{O}})|^2 \approx$ const.
- **Action:**
  - Numerically test uniformity of $\mu_i(k_i)$ for $|A(k)|^2 \propto |k|^{-\alpha}$ in 1D.
  - Dynamically adjust n_{max} in the sum $\sum_n$ until convergence (e.g., new term ¡1
  - Extend to 2D/3D (sum over $\vec{n} \in \mathbb{Z}^m$) to confirm uniformity.

– Test uniformity for exponential/Gaussian spectra. (See repository for code, e.g., 'born$_rule_check.py$').

Document conditions (e.g., large α, specific $f_{s,\mathcal{O}}$) where uniformity (¡5-10

Check if uniformity holds for realistic $f_{s,\mathcal{O}}$ values (e.g., $\bar{f}_s \approx \kappa/\hbar$).

1.1.4: Derivation 9.5 (Convergence Dynamics) Verification

- **Context:** ODE system $\frac{df_{s,i}}{dt} = \eta \sum_j W_{ij}(f_{s,j} - f_{s,i})$ is claimed to lead to $f_{s,i} \to \bar{f}_s$.
- **Action:**
  - Analytically verify for $N = 2$.
  - Numerically solve for $N = 10$ using 'scipy.integrate.solve$_ivp$'.$Testwithphysicallymotivated$W (e.g., $W_{ij} \propto E_i E_j / r_{ij}^2$) and distance-based models. (See repository for code, e.g., 'convergence$_sim.py$').

– Compute graph Laplacian eigenvalues to quantify convergence rates.

Ensure W_{ij} normalization prevents numerical instability.

Validate that $\bar{f}_s$ is insensitive to initial conditions for realistic networks.

2.0.2 Phase 1.2: Development and Analysis of Numerical Toy Models (Months 2-5)

Objective: Implement numerical simulations to test aliasing and emergent quantum phenomena, validating the framework's core hypothesis that sampling leads to quantum-like behavior. **Tools**: Python with NumPy, SciPy (FFTW for FFTs), Matplotlib; Jupyter Notebooks; GitHub. **Deliverable**: Simulation report with plots/animations, shared via GitHub and preprint.

1.2.1: Aliasing Simulation

- **Context:** Test Map$_{\text{Alias}}$ to confirm that sampling $\mathbb{X}_{potential}$ produces quantum-like wavefunctions.

- **Action:**
  - Define 1D $\mathbb{X}_{potential}$ $\Phi(z)$ from $|A(k)|^2 \propto |k|^{-\alpha}$ with random phases.
  - Apply $\text{Map}_{\text{Alias}}$ by band-limiting $\Phi_k(k)$ to $|k| \leq f_{s,\mathcal{O}}/2$ in Fourier space (using FFT/IFFT).
  - Quantify the "wavelength" in $|\psi_{\mathcal{O}}(x)|^2$ via autocorrelation or Fourier analysis to confirm scaling with $f_{s,\mathcal{O}}$.
- Test with deterministic phases ($\theta_k = 0$) for clarity in initial runs. (See repository for code, e.g., 'aliasing$_s im.py$').

> Verify that band-limited $\psi_{\mathcal{O}}$ exhibits quantum-like oscillations.
>
> Mitigate FFT boundary effects using a larger domain or windowing.

1.2.2: Double-Slit Experiment Simulation

- **Context:** Simulate interference (Fig. 3) to verify $\Delta x \propto 1/f_{s,\mathcal{O}}$.
- **Action:**
  - Model $\Phi(z)$ as two Gaussian wavepackets. Apply $\text{Map}_{\text{Alias}}$.
  - Introduce a conceptual screen distance L_{screen} to relate fringe spacing $\Delta x \sim \frac{2\pi}{k_{max}} \frac{L_{screen}}{d_{slits}}$ where $k_{max} \sim f_{s,\mathcal{O}}/2$.
- Perform parameter sweeps for slit separation d_{slits}, packet width σ, and $f_{s,\mathcal{O}}$. (See repository for code, e.g., 'double$_s lit_s im.py$').

> Ensure sufficient grid resolution for narrow Gaussians.
>
> Validate fringe spacing against analytical predictions.

1.2.3: Convergence Model Simulation

- **Context:** Extend analysis of observer network convergence (Fig. 2).
- **Action:**
  - Simulate for $N = 10 - 100$ observers using ODE solver.
  - Test with varied W_{ij} models, including scale-free or small-world network topologies (e.g., using 'networkx').
  - Quantify convergence time (e.g., via variance of $f_{s,i}(t)$).
- Use realistic $f_{s,\mathcal{O}}$ ranges (e.g., $\sim 10^4$ Hz for qubits, $\sim 10^{20}$ Hz for particles) to test convergence towards $\bar{f}_s \approx \kappa/\hbar$. (See repository for code, e.g., 'convergence$_l arge N_s im.py$').

Monitor numerical stability for large N.

Analyze how network topology affects $\bar{f}_s$ and stability.

2.1 Collaboration Plan (Refined)

Crucial for verifying derivations (especially Phase 1.1, Sec. 2.0.1) and executing experiments:

- **Core Team**: Theoretical/mathematical physicists, computational modelers.
- **Needed Expertise**: Experts listed in Sec. 2.1 are essential. Specific outreach to groups working on functional analysis (Sobolev spaces, Gaussian measures [3]), quantum foundations (QBism [1], RQM, Constructor Theory), CMB analysis (Planck/Simons Obs./CMB-S4 teams), precision gravity (e.g., Eöt-Wash), qubit coherence, signal processing theory (Nyquist [4], Shannon [5, 6]).
- **Engagement**: Workshops (Target: Q3 Y2, after initial Phase 1 results), shared repositories (GitHub for Phase 1 code and results), conference presentations, direct collaboration invitations.

3 Nomenclature

See Table 1 for key symbols and concepts.

4 The Foundational Postulates

Core assumptions, with mathematical realization proposed/analyzed in Sec. 9.

4.1 The Unmanifested Potential ($\mathbb{X}_{potential}$)

Postulate 4.1. A foundational reality $\mathbb{X}_{potential}$ exists, prior to structured reality, with infinite information capacity (unbounded $\nu_{\mathbb{X}}$), as undifferentiated potentiality. Ontologically, $\mathbb{X}_{potential}$ might be conceived as a pre-geometric, pre-topological state space, akin to a phase space of pure potentiality, from which spacetime and physical laws emerge through observation-mediated actualization.

Table 1: Glossary of Key Symbols and Concepts

Symbol/Concept	Description	Provisional Units / Type
$\mathbb{X}_{potential}$	Underlying potential reality	Concept / Space $H^s(\mathbb{R}^m)$
$\mathcal{O}$	Interacting entity (Observer)	Concept
$f_{s,\mathcal{O}}$	Observer sampling rate	s^{-1} (temporal)
$\nu_{\mathbb{X}}$, $\vec{k}$	Generalized frequency/wave vector in $\mathbb{X}_{potential}$	s, m^{-1}
$\mathrm{Map}_{\mathrm{Alias}}$	Aliasing transformation	Operator / Map
K	Aliasing kernel	Function / Distribution
$\mathbb{R}_{\mathcal{O}}$	Observer's perceived reality	Hilbert Space $\mathcal{H}_{\mathcal{O}} \cong L^2(\mathbb{R}^3)$
$h_{\mathcal{O}}$	Observer's Planck's constant	$\mathrm{J\,s}$
κ	Universal energy scale constant	J ($\approx 8.19 \times 10^{-14}$ J proposed)
$E_{\mathcal{O}}$	Characteristic energy of $\mathcal{O}$	J
$\tau_{\mathcal{O}}$	Coherence time of $\mathcal{O}$ ($\sim 1/f_{s,\mathcal{O}}$)	s
$\psi_{\mathcal{O}}$	Quantum state	State vector $\in \mathcal{H}_{\mathcal{O}}$
$\mathrm{Interact}_{\mathrm{Resolve}}$	Measurement process	Process / Operator ($P_i + \epsilon$)
μ	Measure on $\mathbb{X}_{potential}$ states	Gaussian Measure on H^s
I_{ij}	Mutual information	bit
C_ℓ	CMB Angular Power Spectrum	$\mu\mathrm{K}^2$
$P(k)$	Primordial Power Spectrum	
$g_{\mu\nu}$	Emergent spacetime metric	Tensor
$T_{\mu\nu}$	Emergent stress-energy tensor	Tensor
$\bar{f}_s$	Mean sampling rate (converged)	s^{-1} ($\approx \kappa/\hbar$)
Δy	Interference fringe spacing	m
α (Sec 8.1)	Spectral index for $\lvert A(k)\rvert^2$	(¿ m+2s)
n (Sec 9.1)	Exponent for $f_{s,\mathcal{O}}(a)$ evolution	
η (Sec 8.5)	Convergence rate constant	Units depend on W_{ij}
W_{ij}	Interaction weight in network	Units depend on model
σ_{noise}	Measurement noise amplitude	Depends on quantity
$H^s(\mathbb{R}^m)$	Sobolev Space	Function Space
Γ_i	Decoherence rate	s^{-1}
$\eta(t)$	Noise term in dynamics	State vectors^{-1}
A (Exp. 10.2)	Proportionality const. for excess noise	Hz or $\mathrm{counts/s}$
C (Exp. 10.3)	Decay rate const. for visibility	s^{-1}

4.2 The Interacting Observer ($\mathcal{O}$) and its Intrinsic Sampling Rate ($f_{s,\mathcal{O}}$)

Postulate 4.2. An "Observer" $\mathcal{O}$ actualizes information from $\mathbb{X}_{potential}$, limited by its intrinsic sampling rate $f_{s,\mathcal{O}}$ (resolution threshold $f_{s,\mathcal{O}}/2$).

Conceptualizing the Observer and $f_{s,\mathcal{O}}$: The nature of an "Observer" $\mathcal{O}$ is a critical aspect of this framework. It is provisionally defined as any entity or system capable of interacting with $\mathbb{X}_{potential}$ in a way that resolves information. This definition is intentionally broad and may span a spectrum:

- *Fundamental particles:* Could an electron be considered a rudimentary observer with an extremely high $f_{s,\mathcal{O}}$ related to its Compton frequency or Zitterbewegung? This remains highly speculative.
- *Measuring devices:* A macroscopic apparatus clearly acts as an observer, with its $f_{s,\mathcal{O}}$ potentially related to its temporal resolution, coherence time ($\tau_{\mathcal{O}}$), or characteristic energy scales involved in its detection mechanism ($E_{\mathcal{O}}$).
- *Complex systems (including conscious beings):* These represent hierarchical observers, possibly with adaptable or effective $f_{s,\mathcal{O}}$ values emerging from their structure and interactions (see Sec. 7).

The physical basis of $f_{s,\mathcal{O}}$ is proposed to link to intrinsic properties of $\mathcal{O}$, such as its characteristic energy $E_{\mathcal{O}}$ (via $f_{s,\mathcal{O}} = E_{\mathcal{O}}/\kappa$) or its coherence time $\tau_{\mathcal{O}}$ (via $f_{s,\mathcal{O}} = 1/\tau_{\mathcal{O}}$). The precise determination of $f_{s,\mathcal{O}}$ for different classes of observers and the derivation of these relationships from more fundamental principles are key research challenges (Roadmap Phase 2, see Sec. **??**). The framework suggests $f_{s,\mathcal{O}}$ is not necessarily fixed but could be dynamic or context-dependent for complex observers.

4.3 Principle 1: Emergence of Observer-Specific Quantum Reality ($\mathbb{R}_{\mathcal{O}}$) and Planck's Constant ($h_{\mathcal{O}}$)

Principle 4.1. $\mathcal{O}$'s reality $\mathbb{R}_{\mathcal{O}}$ (represented by a Hilbert space $\mathcal{H}_{\mathcal{O}}$) emerges via aliasing ($\text{Map}_{\text{Alias}}$) of $\mathbb{X}_{potential}$ constrained by $f_{s,\mathcal{O}}$. The quantum nature and apparent finiteness of information in $\mathbb{R}_{\mathcal{O}}$ are consequences of this sampling limit.

Consequences (Analytical derivations/proposals in Sec. 9):

- **Quantum Formalism:** Proposed $\text{Map}_{\text{Alias}}$ generates Hilbert space $\mathcal{H}_{\mathcal{O}}$ (Derivation 9.2, detailed verification in Sec. 2.0.1). Effective Hamiltonians governing evolution within $\mathbb{R}_{\mathcal{O}}$ are hypothesized to arise from the structure of $\text{Map}_{\text{Alias}}$ and the statistics of $\mathbb{X}_{potential}$, leading to Schrödinger-like or Dirac-like equations in appropriate limits (Roadmap Phase 3).

- **Superposition/Interference:** Emerge from mapping ambiguity and aliased phases (Derivation 9.2, toy model demonstration in Sec. 2.0.2).
- **Resolution of Divergences:** The $f_{s,\mathcal{O}}$-limit provides a natural, observer-dependent UV cutoff.
- **Emergence of $h_{\mathcal{O}}$:** An observer-specific Planck's constant $h_{\mathcal{O}} = \kappa / f_{s,\mathcal{O}}$ is proposed (Proposal 9.3). The framework predicts that $h_{\mathcal{O}}$ can be significantly larger than the shared $\hbar$ for observers with low $f_{s,\mathcal{O}}$. This large $h_{\mathcal{O}}$ is hypothesized to primarily manifest as an increased fundamental resolution limit or "sampling noise" for that observer, affecting decoherence rates or the precision of measurements (see Sec. 10.2), rather than universally re-quantizing all observed phenomena with this larger value. The established energy levels of systems like atoms are presumed to be governed by the converged $h_{\text{shared}} \approx \hbar$ (Sec. 8).
- **Uncertainty Relations:** Consequence of $f_{s,\mathcal{O}}$-limited resolution (Derivation 9.2).

4.4 Principle 2: Actualization of Information through $f_{s,\mathcal{O}}$-Limited Interaction

Principle 4.2. The transition from a superposition of potential states $\psi_{\text{superposed}}$ (representing aliased ambiguities) to a definite outcome $O_{\mathcal{O},\text{actualized}}$ occurs via a measurement process ($\text{Interact}_{\text{Resolve}}$). This process resolves ambiguities within the constraints imposed by $f_{s,\mathcal{O}}$ and the associated $h_{\mathcal{O}}$. "Collapse" is thus an observer-relative, irreversible acquisition of information.

Speculation Note: *The inherently directional process of information actualization, from the undifferentiated $\mathbb{X}_{potential}$ to the resolved $\mathbb{R}_{\mathcal{O}}$ via $Interact_{Resolve}$, might offer a novel perspective on the thermodynamic or quantum arrow of time, linking it to the ongoing process of reality construction by observers.* **Consequences (Analytical derivations/proposals in Sec. 9):**

- **Constrained Measurement.**
- **Resolution:** Interaction selects an $f_{s,\mathcal{O}}$-distinguishable pattern from the aliased possibilities.
- **Born Rule:** $P_i = |\psi_i|^2$ derived via statistical density of underlying states (Derivation 9.4, uniformity check in Sec. 2.0.1).
- **Irreversibility** arises from macroscopic amplification, decoherence (randomization of aliased phases), and the commitment of information to the observer's state.

5 Emergent Physical Phenomena within $\mathbb{R}_{\mathcal{O}}$

(Proposed formal pathways in Sec. 9.7).

5.1 Emergence of Spacetime

Hypothesis 5.1. Spacetime ($g_{\mu\nu}$) is emergent, relational, from $h_{\mathcal{O}}$-quantized interactions limited by $f_{s,\mathcal{O}}$. Its structure reflects the correlational patterns actualized by observers.

5.2 Emergence of Particles and Forces (Standard Model Analog)

Hypothesis 5.2. Particles are (relatively) stable, propagating aliased patterns or topological defects within $\mathbb{R}_{\mathcal{O}}$; forces are exchanges of mediating patterns; fundamental symmetries reflect constraints imposed by the sampling process and the structure of $\text{Map}_{\text{Alias}}$.

5.3 Emergence of Classicality and Thermodynamics

Hypothesis 5.3. Classicality emerges from decoherence (effective randomization of aliased phases due to interaction with many unresolvable degrees of freedom) and aggregation of quantum systems. Thermodynamics governs the statistics of actualized information and energy flows within $\mathbb{R}_{\mathcal{O}}$.

5.4 Gravity as an Emergent Phenomenon (Reconciling with GR)

Hypothesis 5.4. General Relativity emerges as an effective theory describing how distributions of energy-momentum (themselves aliased patterns) influence the emergent geometry of spacetime, possibly via thermodynamic arguments applied to information horizons defined by $f_{s,\mathcal{O}}$.

6 Addressing Cosmological Questions within $\mathbb{R}_{\mathcal{O}}$

(Proposed tests in Sec. 10).

6.1 The Big Bang

Hypothesis 6.1. The "Big Bang" represents the commencement of large-scale, coherent actualization of reality by a nascent network of observers, rather than a physical singularity in a pre-existing spacetime. It could mark a phase transition in the state of $\mathbb{X}_{potential}$ or the emergence of the first observers capable of establishing a shared h_{shared}.

6.2 Dark Matter and Dark Energy

Hypothesis 6.2. These phenomena may arise from aspects of $\mathbb{X}_{potential}$ that are only weakly coupled to ordinary baryonic observers (and thus their sampling processes), or they could be large-scale manifestations of the actualization dynamics itself, such as residual "sampling noise" or effects of an evolving average sampling rate $\bar{f}_s(t)$.

6.3 Fine-Tuning

Hypothesis 6.3. Apparent fine-tuning of cosmological constants may reflect self-consistency conditions: the parameters of the emergent $\mathbb{R}_{\mathcal{O}}$ must be such that observers ($\mathcal{O}$) capable of perceiving and structuring that reality can exist. This hints at an anthropic or consistency-driven selection from a landscape of possibilities within $\mathbb{X}_{potential}$.

7 The Nature of the Observer and Consciousness (Speculative Extensions)

Speculation Note: *This section remains highly speculative and explores potential extensions of the core framework.*

7.1 Hierarchy of Observers

Hypothesis 7.1. $f_{s,\mathcal{O}}$ may vary dramatically with the complexity and internal organization of the observer. Simple systems might possess very high, fixed $f_{s,\mathcal{O}}$, while complex, adaptive systems (like biological organisms) could exhibit more flexible or hierarchically structured effective sampling rates.

7.2 Consciousness

Speculation Note: *Consciousness could represent a particular mode of interaction with $\mathbb{X}_{potential}$, perhaps characterized by a uniquely high degree of integration of sampled information, or an ability to dynamically modulate its effective $f_{s,\mathcal{O}_{conscious}}$ to access or structure information in novel ways. Qualia (subjective experiences) might be interpreted as the "textures" or qualitative aspects of the information actualized by such a conscious observer from $\mathbb{X}_{potential}$.*

8 Inter-Observer Consistency and Universality

A crucial challenge is to explain the observed universality of physical laws and constants, particularly Planck's constant $h \approx \hbar$, if reality is fundamentally observer-dependent.

Hypothesis 8.1. The universality of $h_{\text{shared}} \approx \hbar$ and other physical laws emerges from a convergence process driven by information exchange and interaction within a network of observers (Fig. 2). Dominant scales (e.g., baryonic matter, electromagnetic interactions) and processes (e.g., communication, scientific consensus-building) could drive individual $f_{s,\mathcal{O}}$ values (and thus $h_{\mathcal{O}}$) towards a common, stable equilibrium $\bar{f}_s$, leading to a shared, effective $h_{\text{shared}} = \kappa/\bar{f}_s \approx \hbar$.

9 Proposed Mathematical Formalization

This section presents refined mathematical proposals and analytical derivations (provided by user) intended to formalize the framework. Verification is key future work (Roadmap Sec. 2, especially Phase 1.1 detailed in Sec. 2.0.1).

9.1 Defining $\mathbb{X}_{potential}$ (Ref: Sec. 4.1)

Proposal 9.1 (Field Model with Sobolev Space)**.** Model $\mathbb{X}_{potential}$ states as $\Phi(\vec{z}) \in H^s(\mathbb{R}^m)$, $s > m/2$. Fourier decomposition:

$$\Phi(\vec{z}) = \int_{\mathbb{R}^m} A(\vec{k}) e^{i(\vec{k}\cdot\vec{z}+\theta_{\vec{k}})} d^m\vec{k}$$

with spectrum $|A(\vec{k})|^2 \propto |\vec{k}|^{-\alpha}$ where $\alpha > m + 2s$ ensures Sobolev norm finiteness. A Gaussian measure μ on H^s with covariance $C(\vec{z}_1, \vec{z}_2) = \int |\vec{k}|^{-\alpha} e^{i\vec{k}\cdot(\vec{z}_1-\vec{z}_2)} d^m\vec{k}$ defines statistics.

Derivation 9.1 (Measure Consistency)**.** The Gaussian measure μ is well-defined if the covariance operator C is trace-class ($\mathrm{Tr}(C) = \int |\vec{k}|^{-\alpha} d^m\vec{k} < \infty \implies \alpha > m$) and the measure integrates to 1 over the space ($\int \|\Phi\|^2_{H^s} d\mu(\Phi) < \infty$, requires $\alpha > m + 2s$). The characteristic functional is $\chi(f) = \exp(-\frac{1}{2}\langle f, Cf\rangle)$.

Proposal 9.2 (Graph Model)**.** Alternative: States $\Phi : \mathcal{V} \to \mathbb{C}$ on infinite graph $\mathcal{G}$. Frequencies from Laplacian spectrum.

9.2 Defining $\mathrm{Map}_{\mathrm{Alias}}$ and Emergence of $\mathbb{R}_{\mathcal{O}}$ (Ref: Sec. 4.3)

Derivation 9.2 (Hilbert Space and Interference via Kernel K)**.** Define $\mathrm{Map}_{\mathrm{Alias}}$ projecting $\Phi \in H^s(\mathbb{R}^m)$ to $\psi_{\mathcal{O}} \in \mathcal{H}_{\mathcal{O}} \cong L^2(\mathbb{R}^3)$:

$$\psi_{\mathcal{O}}(\vec{x}) = \int_{\mathbb{R}^m} K(\vec{x}, \vec{z}; f_{s,\mathcal{O}}) \Phi(\vec{z}) d^m\vec{z}$$

With kernel $K(\vec{x}, \vec{z}; f_{s,\mathcal{O}}) = \int_{|\vec{k}|\le f_{s,\mathcal{O}}/2} e^{i\vec{k}\cdot(\vec{x}-\vec{z}_{proj})} \frac{d^m\vec{k}}{(2\pi)^m}$, we obtain:

$$\psi_{\mathcal{O}}(\vec{x}) \propto \int_{|\vec{k}|\le f_{s,\mathcal{O}}/2} A(\vec{k}) e^{i(\vec{k}\cdot\vec{x}+\theta_{\vec{k}})} d^m\vec{k}$$

Hilbert Space Proof: (1) Linearity holds. (2) $\psi_{\mathcal{O}}$ is complex. (3) $\psi_{\mathcal{O}} \in L^2(\mathbb{R}^3)$ (band-limited). (4) Space is complete. Thus $\mathcal{H}_{\mathcal{O}}$ is a Hilbert space. **Interference Proof:** Double-slit yields $|\psi_1 + \psi_2|^2$ containing interference term $2\,\mathrm{Re}(\psi_1^*\psi_2) \propto \cos(\vec{k}_{\mathrm{eff}} \cdot \Delta\vec{z})$. Fringe spacing $\Delta y \propto 1/f_{s,\mathcal{O}}$ (if spatial rate). **Uncertainty Principle:** Band-limiting implies $\delta x \delta k \gtrsim 1$. With $p = (h_{\mathcal{O}}/2\pi)k$, gives $\delta x \delta p \gtrsim h_{\mathcal{O}}/2\pi$.

9.3 Defining $f_{s,\mathcal{O}}$ and Deriving $h_{\mathcal{O}}$ (Ref: Sec. 4.2)

Proposal 9.3 ($f_{s,\mathcal{O}}$ Models and κ Estimation)**.** Propose: (1) $f_{s,\mathcal{O}} = E_{\mathcal{O}}/\kappa$ or (2) $f_{s,\mathcal{O}} = 1/\tau_{\mathcal{O}}$. Conceptual derivation $h_{\mathcal{O}} = \kappa/f_{s,\mathcal{O}}$ identifies κ as a fundamental constant representing energy per resolvable distinction or action per sampling cycle. **Estimating κ:** Adopt $\kappa \approx m_e c^2 \approx 8.19 \times 10^{-14}\,\text{J}$ based on the hypothesis that this energy scale is relevant for the stability and interactions of baryonic matter, which in turn drives the convergence to h_{shared} (Sec. 9.6). This implies the converged rate is $\bar{f}_s \approx \kappa/\hbar \approx 1.24 \times 10^{20}\,\text{Hz}$. For a qubit (e.g., $f_{s,\mathcal{O}} \approx 10^4\,\text{Hz}$ if linked to a slow experimental control/measurement cycle):

$$h_{\mathcal{O}} = \frac{\kappa}{f_{s,\mathcal{O}}} \approx \frac{8.19 \times 10^{-14}\,\text{J}}{10^4\,\text{Hz}} \approx 8.19 \times 10^{-18}\,\text{J s} \gg \hbar$$

This prediction of a potentially very large $h_{\mathcal{O}}$ for low-f_s systems is a key distinguishing feature of the framework, testable via noise or resolution limit experiments (Sec. 10.2).

Derivation 9.3 ($f_{s,\mathcal{O}}$ Scaling for Thermal Systems)**.** If $f_{s,\mathcal{O}} = 1/\tau_{\mathcal{O}}$ and $\tau_{\mathcal{O}}$ is interpreted as a thermal coherence time, e.g., $\tau_{\mathcal{O}} \propto \hbar/(k_B T)$ for some systems, then $f_{s,\mathcal{O}} \propto k_B T/\hbar$. Comparing this with the alternative model $f_{s,\mathcal{O}} = E_{\mathcal{O}}/\kappa$, and assuming $E_{\mathcal{O}} \propto k_B T$ for a thermal observer, this implies an effective $\kappa_{eff} \propto \hbar$.

9.4 Deriving the Born Rule (Ref: Sec. 4.4)

Derivation 9.4 (Born Rule via Statistical Density)**.** Let $\psi = \sum c_i \phi_i$ be the state in $\mathcal{H}_{\mathcal{O}}$, where ϕ_i are distinguishable outcomes. Assume that the probability P_i of actualizing outcome ϕ_i is proportional to the "measure" or "density" of underlying states in $\mathbb{X}_{potential}$ that alias to ϕ_i when ψ is projected. Specifically, let $\mu(S(\psi) \cap S(\phi_i))$ represent this measure, where $S(\cdot)$ denotes the set of pre-images in $\mathbb{X}_{potential}$. The contribution from $\mathbb{X}_{potential}$ that aliases to a specific component ϕ_i (with Fourier components around $\vec{k}_i$) is related to the power spectrum $|A(\vec{k})|^2$ in the bands $\vec{k}_i + n f_{s,\mathcal{O}}$ (for integer n). If the measurement process samples these underlying configurations proportionally to their density, and if the total aliased power contributing to each ϕ_i (denoted $\mu_i = \sum_n |A(\vec{k}_i + n f_{s,\mathcal{O}})|^2$) is approximately constant or uniform across different outcomes ϕ_i (verified in Proposal 9.4), then the probability P_i becomes proportional to $|c_i|^2$, as $|c_i|^2$ weights the contribution of ϕ_i to ψ.

Proposal 9.4 (Verification of Uniformity Assumption for Born Rule)**.** The aliased power measure $\mu_i = \sum_n |A(\vec{k}_i + n f_{s,\mathcal{O}})|^2$. For a power-law spectrum $|A(k)|^2 \propto |k|^{-\alpha}$, the sum over aliases (for $n \neq 0$) is $\sum_{n\neq 0} |\vec{k}_i + n f_{s,\mathcal{O}}|^{-\alpha}$. If $f_{s,\mathcal{O}}$ is large compared to the scale of variation of $\vec{k}_i$, or if the spectrum $A(k)$ is sufficiently smooth or rapidly decaying, this sum might be weakly dependent on $\vec{k}_i$, making μ_i approximately constant.

Proposal 9.5 (Alternative Path: QBism and Informational Constraints)**.** Adopt a QBist perspective where $P_i = |\langle\phi_i|\psi_{\mathcal{O}}\rangle|^2$ represents an observer's rational subjective probability update upon measurement. The framework could aim to derive the Born rule as a condition for coherent belief updating for an observer whose information acquisition is constrained by $f_{s,\mathcal{O}}$ and the aliasing process.

9.5 Modeling Measurement (Interact$_{\text{Resolve}}$)

Proposal 9.6 (Measurement Dynamics with Noise)**.** Model the measurement process (Interact$_{\text{Resolve}}$) via a Lindblad-like master equation for the observer's density matrix ρ. This equation should incorporate both standard quantum evolution and terms reflecting the $f_{s,\mathcal{O}}$-limited nature of the interaction:

$$\dot{\rho} = -i\frac{[H_{\text{eff}}, \rho]}{\hbar_{\text{eff}}} + \sum_k \gamma_k (L_k \rho L_k^\dagger - \frac{1}{2}\{L_k^\dagger L_k, \rho\}) + \mathcal{L}_{\text{noise}}(\rho; f_{s,\mathcal{O}}, h_{\mathcal{O}})$$

Here, H_{eff} is an effective Hamiltonian. $\hbar_{\text{eff}}$ might be the shared $\hbar$ or influenced by $h_{\mathcal{O}}$ depending on context. The Lindblad operators L_k and decoherence rates γ_k could be $f_{s,\mathcal{O}}$-dependent. For instance, if an outcome ϕ_i has N_i pre-images in $\mathbb{X}_{potential}$ that alias to it, the rate of resolving this ambiguity might be $\Gamma_i \approx f_{s,\mathcal{O}}/N_i$. The term $\mathcal{L}_{\text{noise}}$ represents noise or projection errors inherent in the $f_{s,\mathcal{O}}$-limited sampling, potentially with variance $\sigma^2_{\text{noise}} \propto (h^2_{\mathcal{O}}/\tau_{\text{interaction}})$ or similar scaling, reflecting the "graininess" imposed by $h_{\mathcal{O}}$.

9.6 Modeling Inter-Observer Consistency (Ref: Sec. 8)

Derivation 9.5 (Convergence Dynamics)**.** A simplified model for the evolution of individual sampling rates $f_{s,i}$ in a network of N interacting observers can be given by a system of coupled ODEs:

$$\frac{df_{s,i}}{dt} = \eta \sum_{j=1}^{N} W_{ij}(f_{s,j} - f_{s,i})$$

where η is a rate constant and W_{ij} represents the strength of interaction or information flow between observer i and j. For a connected network (where W_{ij} forms a connected graph) and symmetric weights ($W_{ij} = W_{ji}$), this system typically leads to convergence, $f_{s,i}(t) \to \bar{f}_s$ for all i, where $\bar{f}_s$ is a weighted average of initial rates or a value determined by the network structure and external constraints.

Proposal 9.7 (Justification for $\bar{f}_s \approx \kappa/\hbar$)**.** The converged sampling rate $\bar{f}_s$ is hypothesized to correspond to the shared value $\kappa/\hbar$. This requires a physical basis for the interaction weights W_{ij} and the stability of this particular $\bar{f}_s$. Model interaction weights

based on dominant physical forces, e.g., $W_{ij} \propto \alpha_{EM} E_i E_j / r_{ij}^2$ for electromagnetically interacting observers with characteristic energies E_i, E_j. Hypothesize that the stable equilibrium $\bar{f}_s$ is one that maximizes the stability, information exchange capacity, or persistence of structures predominantly based on baryonic matter (e.g., atoms, molecules). Such structures are fundamentally governed by quantum mechanics with Planck's constant $\hbar$, and their characteristic energy scale is related to $m_e c^2$. If the network dynamics favor an $\bar{f}_s$ that is "resonant" with these structures, it might lead to $\bar{f}_s \approx m_e c^2/\hbar$. For self-consistency with $h_{\text{shared}} = \kappa/\bar{f}_s \approx \hbar$, this would imply $\kappa \approx m_e c^2$.

9.7 Formalizing Emergent Physics (Ref: Sec. 5)

(Long-term goals for Roadmap Phases 3-5).

Proposal 9.8 (Pathways to Emergent Physics)**. Spacetime:** The metric $g_{\mu\nu}$ could emerge from correlators of the observed field $\psi_{\mathcal{O}}$, such as $\langle \psi_{\mathcal{O}}(\vec{x}) \psi^*_{\mathcal{O}}(\vec{y}) \rangle$, or from effective distances on a graph of interacting observers. One tentative proposal is $g_{\mu\nu}(\vec{x}) \approx \int K(\vec{x}, \vec{z}; f_{s,\mathcal{O}}) K^*(\vec{x}, \vec{z}; f_{s,\mathcal{O}}) d^m \vec{z}$ (or a functional thereof), reflecting how the observer's sampling kernel structures the perceived vacuum. **Particles/Forces:** Particles could be (meta)stable eigenmodes, topological defects, or localized persistent patterns of the dynamics governing $\mathbb{R}_{\mathcal{O}}$. Symmetries observed in particle physics might be inherited from symmetries of the sampling kernel K, the underlying graph structure (if using a graph model for $\mathbb{X}_{potential}$), or the aliasing process itself. **Gravity:** An entropic gravity approach [7] could be adapted, where gravity arises from information changes on $f_{s,\mathcal{O}}$-defined holographic screens or observer horizons. The emergent entropy S could scale with an area A measured in units of an observer-dependent fundamental length $l^2_{\mathcal{O}} = (h_{\mathcal{O}} G/c^3)$. **Quantum Dynamics:** As mentioned in Sec. 4.3, the derivation of effective Schrödinger or Dirac equations for particles within $\mathbb{R}_{\mathcal{O}}$ is a primary goal. This would involve showing how operators corresponding to momentum and energy arise from the action of $\text{Map}_{\text{Alias}}$ on $\mathbb{X}_{potential}$, and how their commutation relations (scaled by $h_{\mathcal{O}}$ or $\hbar$) emerge.

10 Proposed Empirical Validation Strategies

Detailed experimental/observational designs to test the framework (Roadmap Phase 5).

10.1 Cosmological Tests: Evolving $f_{s,\mathcal{O}}$

Experiment Design 10.1 (CMB Power Spectrum Analysis)**. Hypothesis:** If the average sampling rate of the "cosmic observer" (or the network of observers defining shared reality) evolves with cosmological scale factor a, such that $f_{s,\text{cosmic}}(a) \propto a^{-n}$, then $h_{\text{cosmic}}(a) = \kappa/f_{s,\text{cosmic}}(a) \propto a^n$. This evolving h could alter the primordial power spectrum $P(k)$ or its transfer function. For instance, if $P(k)$ effectively scales with h, then an $h(a)$ could imprint a scale-dependent feature. A simple model might predict an effective spectral index $n_s' = n_s - 1 + 2n + 1 = n_s + 2n$ if $P(k) \propto k^{n_s-1}(h/h_0)^2$ and $k \propto 1/a$. **Prediction:** For $n = 0.01$, this could lead to a 2**Strategy:** Use MCMC analysis with modified CLASS [8] or CAMB to fit Planck, Simons Observatory, and future CMB-S4 data. Constrain the parameter n. Target precision: $\sigma(n) \approx 0.005$. *Outcome:* A statistically significant constraint or detection of $n \neq 0$ would provide strong evidence for or against this aspect of the model. *Falsification/Constraint:* A null result ($n = 0$ within tight error bars, consistent with standard ΛCDM) would constrain this specific model of evolving h_{cosmic} or imply that any such evolution is too small to be detected with current/near-future instruments.

10.2 Quantum Optics and Condensed Matter Tests

These tests aim to detect effects of a large, observer-specific $h_{\mathcal{O}}$ for systems with relatively low intrinsic sampling rates $f_{s,\mathcal{O}}$. Preparatory simulations are part of Roadmap Phase 5 (see Sec. **??**).

Experiment Design 10.2 (Photon Counting Noise in Qubit Readout)**. Setup:** A superconducting qubit system operating at T=20 mK to 100 mK. The qubit's state is read out by measuring microwave photons in a coupled resonator. Assume the "observer" in this context is the measurement apparatus, whose effective sampling rate $f_{s,\mathcal{O}}$ might be related to its coherence time $\tau_{\mathcal{O}}$ or the inverse of the measurement integration time. For $\tau_{\mathcal{O}} \sim 10\,\mu\text{s}$ to $100\,\mu\text{s}$, $f_{s,\mathcal{O}} \sim 10^4\,\text{Hz}$ to $10^5\,\text{Hz}$. **Hypothesis:** The large $h_{\mathcal{O}} = \kappa/f_{s,\mathcal{O}}$ associated with this $f_{s,\mathcal{O}}$ introduces additional "sampling noise" beyond standard quantum shot noise or thermal noise. **Prediction:** Excess variance in photon counts (or integrated signal) $\sigma^2_{excess} \approx A \cdot \tau_{\mathcal{O}}(T)$, where A is a proportionality constant (units of count rate, e.g., Hz or counts/s, if σ^2 is variance of counts and $\tau_{\mathcal{O}}$ is in seconds). For example, if $A \approx 10^{-3}\langle\dot{N}\rangle$ where $\langle\dot{N}\rangle \sim 10^6\,\text{counts/s}$ is the av-

erage photon detection rate, then $A \sim 10^3\,\mathrm{Hz}$. **Parameters Precision**: Need to measure variance with precision better than 1**Analysis:** Fit the measured total variance $\sigma^2_{total}(T) = \sigma^2_{shot} + \sigma^2_{thermal}(T) + \sigma^2_{detector} + A \cdot \tau_{\mathcal{O}}(T)$. Test the statistical significance of $A > 0$ via likelihood ratio tests or Bayesian model comparison. *Outcome:* Observation of $\tau_{\mathcal{O}}$-dependent excess noise, after accounting for all known noise sources, would support the model. *Falsification/Constraint:* A null result (no excess noise correlated with $\tau_{\mathcal{O}}$ beyond established noise models) would constrain the magnitude of A or challenge the assumed link between $h_{\mathcal{O}}$ and this type of noise. *Alternative Explanations:* If excess noise is found, rigorous investigation will be needed to exclude subtle conventional noise sources (e.g., unmodeled thermal effects, detector instabilities correlated with temperature-dependent parameters) before attributing it to the framework's novel predictions.

Experiment Design 10.3 (Interference Visibility Dependence on Detector Characteristics)**. Setup:** Mach-Zehnder interferometer using single photons (e.g., $1550\,\mathrm{nm}$). The detectors (e.g., superconducting nanowire single-photon detectors - SNSPDs) are cooled to T=$20\,\mathrm{mK}$ to $100\,\mathrm{mK}$. Assume their effective $f_{s,\mathcal{O}}$ is related to their intrinsic recovery time or coherence properties, $\tau_{\mathcal{O}}(T) \sim 10\,\mu\mathrm{s}$ to $100\,\mu\mathrm{s}$. **Hypothesis:** The $f_{s,\mathcal{O}}$-limited resolution of the detector (governed by its $h_{\mathcal{O}}$) could affect its ability to distinguish paths or resolve phase information perfectly, leading to an additional source of visibility degradation. **Prediction:** The interference visibility V exhibits an extra decay factor dependent on the detector's $\tau_{\mathcal{O}}$: $V \propto \exp(-C \cdot \tau_{\mathcal{O}}(T))$, where C is a constant with units of s^{-1}. For example, if $C \approx 10^3\,\mathrm{s}^{-1}$, this predicts a measurable effect. **Parameters:** Path length difference ˜$1\,\mathrm{mm}$ (to ensure coherence of source photons). Photon flux $\sim 10^5\,\mathrm{photons/s}$ to avoid detector saturation but allow sufficient statistics. Accumulate data over many runs (e.g., 100 runs per temperature point). **Analysis:** Measure V as a function of detector temperature T. Fit the data to $V(T) = V_0 \cdot \exp(-\Gamma_{std} L) \cdot \exp(-C \cdot \tau_{\mathcal{O}}(T))$, where V_0 is ideal visibility and $\Gamma_{std} L$ accounts for standard decoherence mechanisms. Test if $C > 0$ significantly. *Outcome:* Detecting a systematic dependence of interference visibility on detector temperature (via $\tau_{\mathcal{O}}(T)$) beyond known mechanisms would support the framework.

10.3 Precision Tests of Gravity

Experiment Design 10.4 (Torsion Balance/Micro-Cantilever Test for Deviations from Newtonian Gravity)**. Setup:** Probe the gravitational force between small test masses (e.g., $m \sim 10^{-3}\,\mathrm{kg}$ to $10^{-6}\,\mathrm{kg}$) at short separations (e.g., $d \sim 1\,\mu\mathrm{m}$ to $100\,\mu\mathrm{m}$) using highly sensitive micro-cantilevers or torsion balances (target sensitivity $\sim 10^{-23}\,\mathrm{N}$ to $10^{-24}\,\mathrm{N}$). **Hypothesis:** If spacetime is emergent and its "granularity" is related to an observer-dependent Planck length $l_{\mathcal{O}} = \sqrt{h_{\mathcal{O}} G/c^3}$, then deviations from Newto-

nian/GR gravity might appear at scales related to $l_{\mathcal{O}}$. The $f_{s,\mathcal{O}}$ (and thus $h_{\mathcal{O}}$) for the experimental apparatus itself could be relevant. **Prediction:** A potential deviation ΔF from the expected force F_{Newton} could scale as $\Delta F \propto (l_{\mathcal{O}}/d)^p F_{Newton}$ for some power p (e.g., $p = 2$).

- If $f_{s,\mathcal{O}}$ for the apparatus at $300\,\mathrm{K}$ is thermally determined, $f_{s,\mathcal{O}} \approx k_B T/\kappa$. Using $\kappa \approx m_e c^2 \approx 8.19 \times 10^{-14}\,\mathrm{J}$, then $f_s(300\,\mathrm{K}) \approx (1.38 \times 10^{-23}\,\mathrm{J\,K^{-1}} \cdot 300\,\mathrm{K})/8.19 \times 10^{-14}\,\mathrm{J} \approx 5.06 \times 10^{-8}\,\mathrm{Hz}$. This gives an enormous $h_{\mathcal{O}} = \kappa/f_s \approx 1.62 \times 10^{-6}\,\mathrm{J\,s}$, and $l_{\mathcal{O}} \approx 7.77 \times 10^{-13}\,\mathrm{m}$. For $d = 1\,\mu\mathrm{m}$ and $p = 2$, $\Delta F/F_N \sim (l_{\mathcal{O}}/d)^2 \sim (7.77 \times 10^{-13}10^{-6}\,)^2 \sim 6 \times 10^{-13}$. If $F_N \sim Gm^2/d^2 \sim 6.67 \times 10^{-11} \cdot (10^{-6}\,)^2/(10^{-6}\,)^2 \sim 6.67 \times 10^{-11}\,\mathrm{N}$ (for $m = 1\,\mu\mathrm{g}$), then $\Delta F \sim 4 \times 10^{-23}\,\mathrm{N}$.

- If $f_{s,\mathcal{O}}$ is determined by gravitational dynamics of the test masses themselves, e.g., $f_{s,\mathcal{O}} \sim \sqrt{Gm/d^3}/\kappa$ (highly speculative scaling), for $m = 10^{-6}\,\mathrm{kg}$, $d = 10^{-5}\,\mathrm{m}$, $f_s \sim 2.58 \times 10^{-3}\,\mathrm{Hz}$ (using $\kappa = 1$) or much higher if κ is small. If $f_s \sim 3.16 \times 10^5\,\mathrm{Hz}$ (as in original text, source unclear), $h_{\mathcal{O}} \approx 2.59 \times 10^{-19}\,\mathrm{J\,s}$, $l_{\mathcal{O}} \approx 2.46 \times 10^{-27}\,\mathrm{m}$, leading to $\Delta F/F_N \sim (2.46 \times 10^{-27}10^{-5}\,)^2 \sim 6 \times 10^{-44}$, which is unobservable.

The thermal f_s model yields a potentially detectable deviation with next-generation experiments. **Analysis:** Carefully measure force $F(d)$ and fit to $F_{GR}(d) + F_{Casimir}(d) + F_{other\_known} + \delta F_{model}(d, l_{\mathcal{O}})$. Meticulous control of systematic effects (e.g., Casimir forces via material choice and graphene shielding, electrostatic forces) is paramount. *Outcome:* A statistically significant deviation consistent with a model based on $l_{\mathcal{O}}$ would provide strong support for emergent spacetime linked to an observer-dependent $h_{\mathcal{O}}$.

10.4 Astrophysical Signatures (Dark Matter/Dark Energy Analogs)

Experiment Design 10.5 (Observational Constraints on DM/DE Analogs)**. Strategy:**

- **Dark Matter Analogs**: If DM-like effects arise from modes of $\mathbb{X}_{potential}$ that are sampled very weakly or with a very low effective $f_{s,DM}$, this could lead to gravitational effects without corresponding luminous matter. The framework might predict specific galactic core profiles (e.g., shallower than standard CDM, potentially like $\rho(r) \propto r^{-0.5}$ as in Derivation 10.1) or modified interaction cross-sections for these "unresolved" components of $\mathbb{X}_{potential}$. Test these predictions against data from Rubin Observatory (LSST), JWST galaxy dynamics, large-scale structure surveys, and CMB lensing.

- **Dark Energy Analogs**: If the accelerated expansion of the universe is related to the dynamics of actualization, e.g., an evolving average sampling rate $\bar{f}_s(t)$ for the cosmic observer network, this could manifest as a specific equation of state for dark energy $w(a)$. For example, if the "energy density" of the actualization

process scales as f_s^x and $f_s \propto a^{-n}$, this could lead to $w(a) = w_0 + w_a(1-a)$ with specific relations between w_0, w_a and n, x. For instance, if effective DE density $\rho_{DE} \propto f_s^{-1} \propto a^n$, then $w = -(1 + n/3)$ if n is small. Constrain such models using data from DESI BAO, Euclid weak lensing, and Roman Space Telescope SNe Ia.

Outcome: Consistency of specific predictions derived from the sampling framework with astrophysical observations would support its potential to explain DM/DE phenomena.

Derivation 10.1 (DM Profile from Low-f_s Modes)**.** Hypothesize that Dark Matter-like gravitational effects arise from components of $\mathbb{X}_{potential}$ that are characterized by a very low intrinsic sampling rate $f_{s,DM}$ by baryonic observers, or are themselves "observers" with such low f_s. If the process of gravitational clustering and structure formation is affected by the sampling rate (e.g., through an effective $h_{DM} = \kappa/f_{s,DM}$ influencing the de Broglie wavelength or phase space density), this could lead to different density profiles than standard Cold Dark Matter. For example, a very large effective h_{DM} might suppress small-scale power or lead to cored profiles (e.g., $\rho(r) \propto r^{-\gamma}$ with $\gamma < 1$ at small r) due to quantum-like pressure effects on larger scales. Detailed N-body simulations incorporating such f_s-dependent physics would be required to derive specific predictions.

11 Illustrative Diagrams

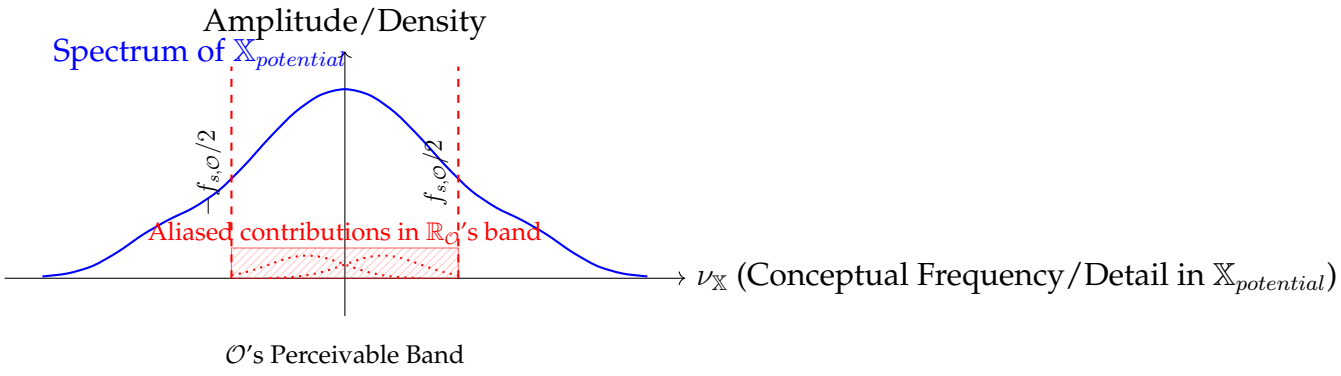

Figure 1: Conceptual illustration of aliasing via $\text{Map}_{\text{Alias}}$ (Sec. 9.2). High-$\nu_{\mathbb{X}}$ components (blue) from the underlying potential fold into $\mathcal{O}$'s perceivable band ($\pm f_{s,\mathcal{O}}/2$), contributing to the perceived reality $\mathbb{R}_{\mathcal{O}}$ (red). This is analogous to the stroboscopic "wagon wheel" effect. (Target of Roadmap Phase 1.2, Sec. 2.0.2)

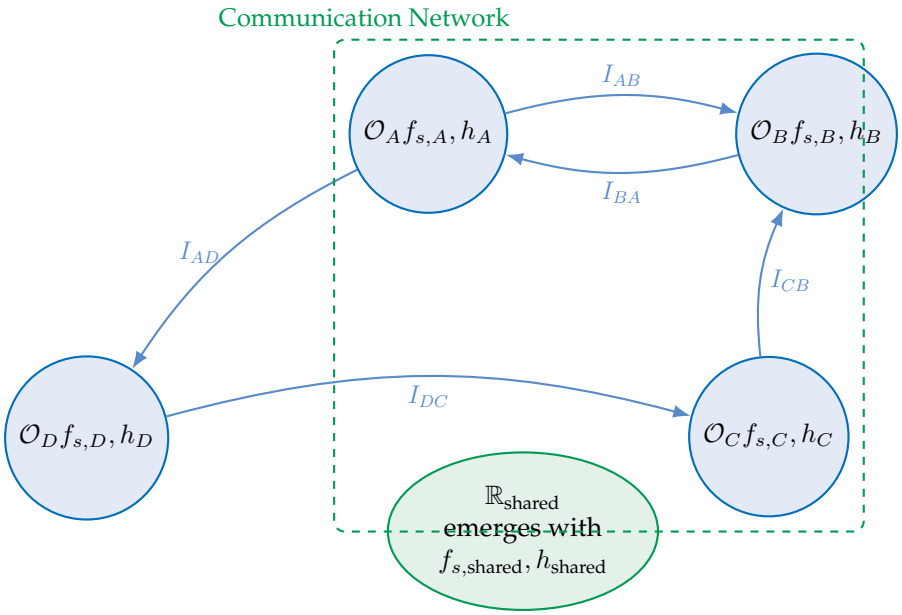

Figure 2: Network of observers $\mathcal{O}_i(f_{s,i}, h_i)$. Mutual interaction and information exchange (I_{ij}) drive convergence of individual sampling parameters towards a shared reality $\mathbb{R}_{\text{shared}}$ characterized by $f_{s,\text{shared}}$ and $h_{\text{shared}} \approx \hbar$. (Analyzed in Derivation 9.5; Target of Roadmap Phase 1.1/1.2, Sec. 2.0.1 2.0.2, and Phase 4)

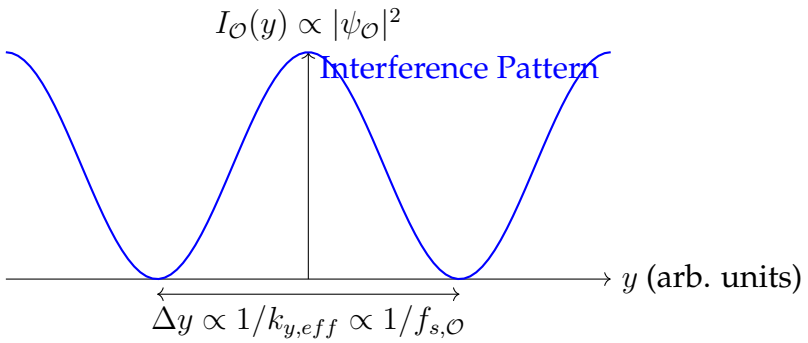

Figure 3: Analytical double-slit interference pattern $I_{\mathcal{O}}(y)$ emerging from $\text{Map}_{\text{Alias}}$ (Derivation 9.2). The fringe spacing Δy scales inversely with the effective spatial sampling rate (or the momentum resolution limit set by $f_{s,\mathcal{O}}$ and $h_{\mathcal{O}}$), supporting the emergence of quantum wave-like behavior. (Target of Roadmap Phase 1.1/1.2, Sec. 2.0.1 2.0.2, and Phase 3)

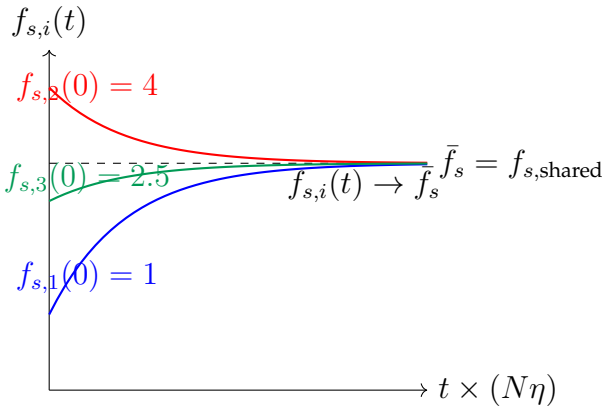

Figure 4: Analytical trajectories $f_{s,i}(t) \to \bar{f}_s$ from the ODE solution (Derivation 9.5), illustrating convergence of individual observer sampling rates towards a common shared rate $f_{s,\text{shared}}$ in an interacting network. (Target of Roadmap Phase 1.1/1.2, Sec. 2.0.1 2.0.2, and Phase 4)

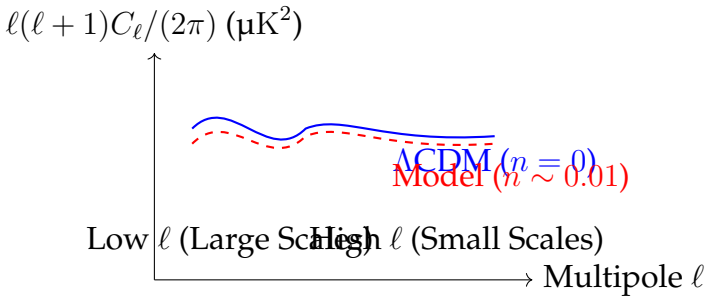

Figure 5: Predicted CMB C_ℓ modification (e.g., suppression) at low ℓ for an evolving $h_{\mathcal{O}}(t)$ (parameterized by $n \sim 0.01$) compared to standard ΛCDM (where $n = 0$). The exact shape of modification depends on the detailed model. (Experiment 10.1)

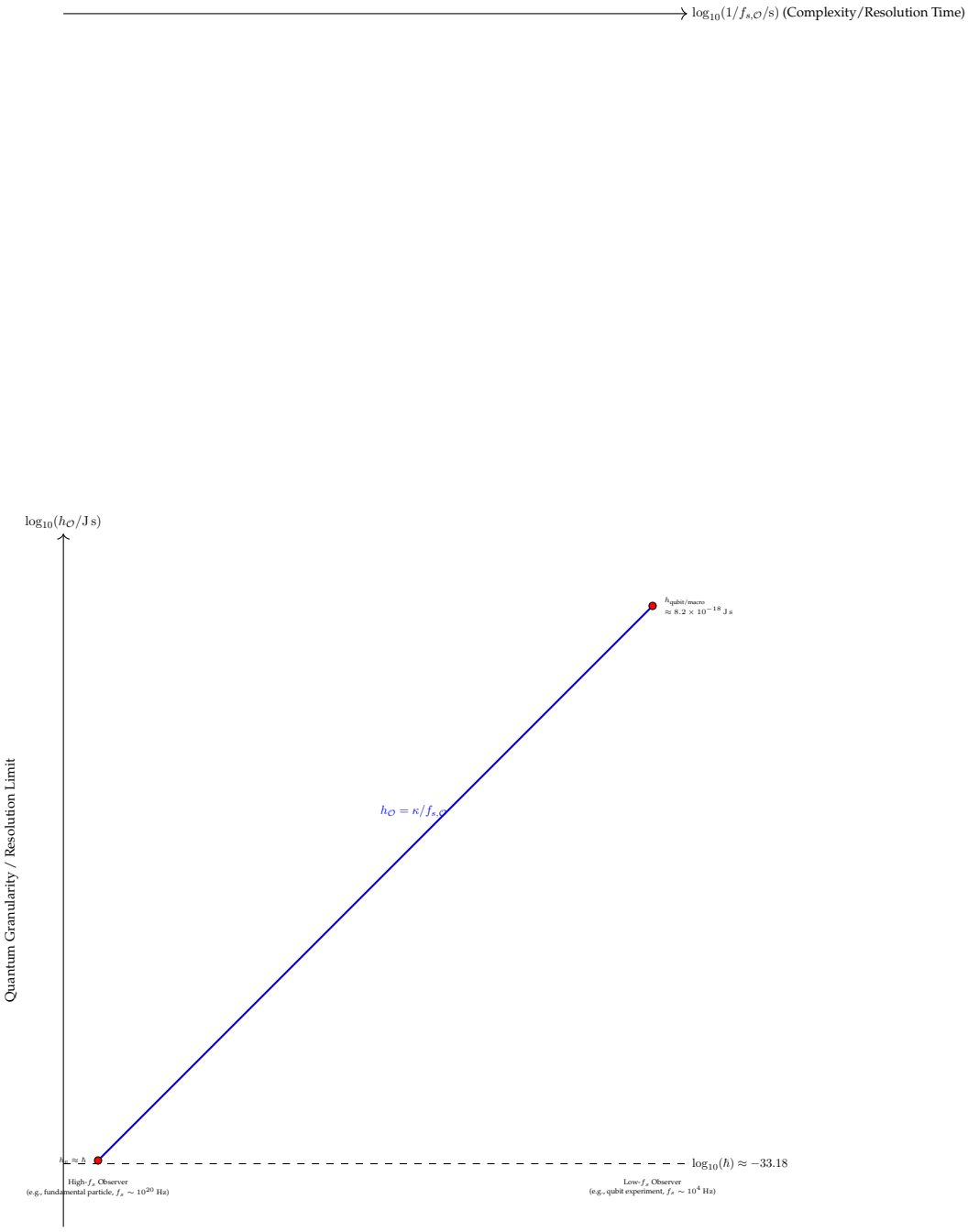

Figure 6: Schematic log-log plot illustrating the proposed inverse relationship between an observer's effective Planck's constant $h_{\mathcal{O}}$ and its sampling rate $f_{s,\mathcal{O}}$ (where $1/f_{s,\mathcal{O}}$ can be seen as a measure of complexity or characteristic resolution time). The plot uses $\kappa \approx m_e c^2 \approx 8.19 \times 10^{-14}$ J. Observers with lower $f_{s,\mathcal{O}}$ (higher complexity/slower characteristic time) would experience a reality with a larger effective $h_{\mathcal{O}}$. The convergence mechanism (Sec. 9.6) is crucial for explaining why the shared physical reality is characterized by $h_{\text{shared}} \approx \hbar$, corresponding to a very high converged sampling rate $\bar{f}_s \approx \kappa/\hbar$. (Based on Proposal 9.3)

12 Conclusion: Towards a Participatory, Information-Limited, and Unified Cosmology

This document has detailed the "Participatory Universe" framework, a conceptual model where experienced reality emerges for observers via an $f_{s,\mathcal{O}}$-limited sampling of an underlying, unmanifested potential, $\mathbb{X}_{potential}$. Key quantum phenomena, including the structure of Hilbert space, superposition, interference, and an observer-specific Planck's constant $h_{\mathcal{O}}$, are hypothesized to arise from the process of aliasing inherent in this finite sampling. Specific analytical derivations (Sec. 9) and detailed empirical tests (Sec. 10) have been proposed to guide the rigorous development and validation of this framework, structured by the Research Roadmap (Sec. 2), with immediate actions for Phase 1 detailed in Sec. 2.0.1 and Sec. 2.0.2.

The core implications of this framework are profound:

- Quantum Mechanics is posited as an emergent theory of information, shaped by the observational limits of interacting entities.
- Planck's constant $h_{\mathcal{O}}$ is observer-relative, with the universal $\hbar$ emerging as a converged value within a network of interacting observers.
- Classical divergences find a natural resolution through the inherent UV cutoff provided by $f_{s,\mathcal{O}}$.
- A path towards a unified description of physical phenomena, including spacetime, particles, and forces, is envisioned as emergent properties of the sampling process.
- The universe is fundamentally participatory, its manifested form co-created by the act of observation, echoing Wheeler's "it from bit" [2].

While sharing conceptual ground with observer-centric interpretations like QBism [1] (which emphasizes the agent's role in probability assignment) and Relational Quantum Mechanics (where properties are defined by interactions), this framework uniquely proposes a specific physical mechanism – sampling and aliasing from a deeper potentiality – as the origin of quantum formalism and an observer-dependent $h_{\mathcal{O}}$. It also seeks to provide a pathway for the emergence of spacetime and particles, aiming for a more comprehensive physical ontology.

Successfully executing the proposed analytical derivations and empirical experiments is paramount. This document serves as a detailed prospectus and research plan, inviting critical scrutiny and collaboration from the broader scientific community to investigate whether the act of "sampling" indeed underpins the fabric of reality.

The challenges are significant, including the rigorous definition of the observer across scales, the precise origin of κ and $f_{s,\mathcal{O}}$, the reconciliation with relativistic principles, and the derivation of the Standard Model and General Relativity. However, the potential to address long-standing foundational questions in physics provides a strong impetus for this ambitious endeavor.

References

[1] Christopher A. Fuchs and Blake C. Stacey. Qbism: Quantum theory as a hero's handbook. *arXiv preprint arXiv:1612.07308*, 2016.

[2] John Archibald Wheeler. *Information, Physics, Quantum: The Search for Links*. Addison-Wesley, Redwood City, CA. Appeared in "Complexity, Entropy, and the Physics of Information", SFI Studies in the Sciences of Complexity, Vol. VIII, 1990.

[3] Vladimir Igorevich Bogachev. *Gaussian measures*, volume 62. American Mathematical Soc., 1998.

[4] Harry Nyquist. Certain topics in telegraph transmission theory. *Transactions of the American Institute of Electrical Engineers*, 47(2):617–644, 1928.

[5] Claude E Shannon. Communication in the presence of noise. *Proceedings of the IRE*, 37(1):10–21, 1949.

[6] Claude E Shannon. A mathematical theory of communication. *The Bell system technical journal*, 27(3):379–423, 1948.

[7] Erik P. Verlinde. On the origin of gravity and the laws of newton. *Journal of High Energy Physics*, 2011(4):29, 2011.

[8] Julien Lesgourgues. The cosmic linear anisotropy solving system (class) i: Overview. *arXiv preprint arXiv:1104.2932*, 2011.